

CONF-950846--57

SAND95-2058C

RETURN TO THE SHORTED AND SHUNTED QUARTZ GAUGE PROBLEM: ANALYSIS WITH THE SUBWAY CODE*

S. T. Montgomery, R. A. Graham, and M.U. Anderson

Sandia National Laboratories, Albuquerque, NM 87185

Simulations with finite element models of well controlled impact experiments with x-cut quartz gauges have been performed with the transient electromechanics code SUBWAY. Comparisons of measured gauge output current with calculated output current were made for four fully-electroded gauge configurations, involving two different can spacings and potting materials. The observed good agreement between measured and calculated currents provides a basis for confidence in the basic capabilities of the code.

INTRODUCTION

Quartz gauges have the ability to provide high fidelity measurements of impulsive stress pulses in materials with resolution of a few nanoseconds. Although the conditions under which the gauges can provide well defined measurements were carefully delineated in early work¹, requirements for measurements in difficult environments have led investigators to use gauge configurations which invoke two-dimensional mechanical and electrical conditions in the gauges. With the development of the transient electrodynamics code SUBWAY these conditions can now be accurately simulated and used to identify critical features of gauge responses.

Of particular interest at present is the measurement of the time-resolved stress states produced in materials by intense, short duration, soft x-rays produced by the Saturn accelerator at Sandia National Laboratories. (See paper by Barrett, et. al., present proceedings.) Three gauge configurations, as indicated in Fig. 1, are being investigated including the shunted guard ring gauge (A), the fully-electroded gauge (B), and the shorted-guard ring gauge (C).

To better understand the responses of fully electroded and shorted guard ring gauges we used the SUBWAY code with finite element models to simulate responses for several well controlled experiments.

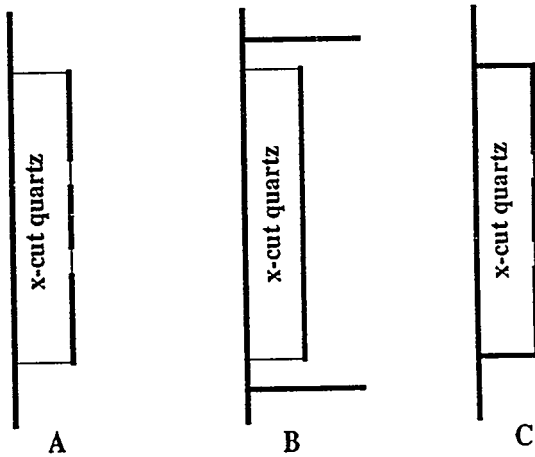


FIGURE 1. Typical Quartz Gauge Configurations.

EXPERIMENTAL

Controlled, precisely characterized impact loading experiments were carried out on the Sandia Precision Impact Loading Facility. As has been the case in prior work, the well-aligned

* This work supported by the United States Department of Energy under contract DE-AC04-94AL8500.

DISCLAIMER

This report was prepared as an account of work sponsored by an agency of the United States Government. Neither the United States Government nor any agency thereof, nor any of their employees, makes any warranty, express or implied, or assumes any legal liability or responsibility for the accuracy, completeness, or usefulness of any information, apparatus, product, or process disclosed, or represents that its use would not infringe privately owned rights. Reference herein to any specific commercial product, process, or service by trade name, trademark, manufacturer, or otherwise does not necessarily constitute or imply its endorsement, recommendation, or favoring by the United States Government or any agency thereof. The views and opinions of authors expressed herein do not necessarily state or reflect those of the United States Government or any agency thereof.

DISCLAIMER

**Portions of this document may be illegible
in electronic image products. Images are
produced from the best available original
document.**

impact of X-cut quartz disks at impact velocities known to 0.1% provided the loadings. The tilt was typically less than 200 μ radian. Short circuited current pulses were measured with low ohmic value current shunts connected to high frequency digitizers with low loss cables. Disks were all 37 mm in diameter and 6.35 mm thick.

COMPUTATIONAL

SUBWAY is a transient electromechanics code developed at Sandia National Laboratories⁶. The code uses a finite element description to model the motion and electric displacement in charge-free materials, as governed by Cauchy's equation of motion and Gauss's law. Using the electric field-electric potential relation, $\mathbf{E} = -\text{grad } \phi$, and the constitutive relation for the electric displacement in Gauss's law provides a Poisson equation governing the electric potential. Here \mathbf{E} is the electric field and ϕ is the electric potential.

A complete description of assumptions and solution method used in SUBWAY has been given by Montgomery and Chavez.² Material motion is advanced over a time step Δt using standard methods³ of explicit time integration with artificial viscosity to smooth discontinuities. Prior to updating the stress tensor at end of a time step, the Poisson equation governing the electric potential is solved using a conjugate gradient method and the electric field in materials calculated using the electric field-electric potential relation. New values for the stress tensor and electric displacement can then be evaluated using constitutive relations appropriate to materials involved in the simulation.

SUBWAY has the capability to treat general electrical loading conditions on specified surfaces. In particular, the integral form of Gauss's law is used to calculate the electric charge, Q , on a specified electrode or conducting surface at each

⁶ SUBWAY code was developed primarily by S.T. Montgomery, P. F. Chavez, and L. M. Taylor at Sandia National Laboratories. It is not generally available.

time step of the simulation. The electric current, I , flowing from the electrode can then be calculated using the finite difference relation,

$$I = - (Q^{n+1} - Q^n) / \Delta t.$$

Quartz has one threefold axis with two twofold axes normal to it. One of the twofold axes corresponds to the cylindrical axis about which a disk of x-cut quartz is fabricated. Linear piezoelectric constitutive relations for x-cut quartz are given by Tiersten.⁴ Graham⁵ has shown that an accurate description of impacting x-cut quartz requires addition of nonlinear terms to the linear piezoelectric constitutive relations. In this study, selected higher order terms are included in the constitutive relations for the normal component of stress in the x-direction T_{xx} and the electric displacement vector \mathbf{D} . We take

$$T_{xx} = \tilde{T}_{xx} + \frac{1}{2} c_{1111}^E S_{xx}^2 + \frac{1}{6} c_{11111}^E S_{xx}^3 - \frac{1}{2} e'_{111} E_x$$

$$D_x = \tilde{D}_x + \frac{1}{2} e'_{111} S_{xx}^2 + \epsilon'_{xx} \text{tr}(\mathbf{S}) E_x$$

where \tilde{T}_{xx} and \tilde{D}_x are linear piezoelectric stress and electric displacement components, respectively, while S_{xx} and $\text{tr}(\mathbf{S})$ are the normal component of the strain in the x-direction and trace of the strain tensor, respectively. The constants c_{1111}^E , c_{11111}^E , e'_{111} , and ϵ'_{xx} , are associated with nonlinear material response and have been discussed by Graham. The dependence of dielectric constant on material density through the trace of the strain tensor is also incorporated into the Y and Z components of the electric displacement.

RESULTS

We performed simulations of experiments on several fully-electroded gauge configurations. The configuration used in the simulations is shown in Fig. 2. The figure shows a quarter section of the impactor, the gauge, and the backing aluminum tamper surrounded by potting and an aluminum can. The simulation shows electric field

distributions about 0.7 μ second after impact. The one-dimensional conditions in the center of the gauge disk, and the two-dimensional field distributions in the outer portion of the disk are clearly indicated. The can is spaced at $L/2$, where L is the gauge thickness.

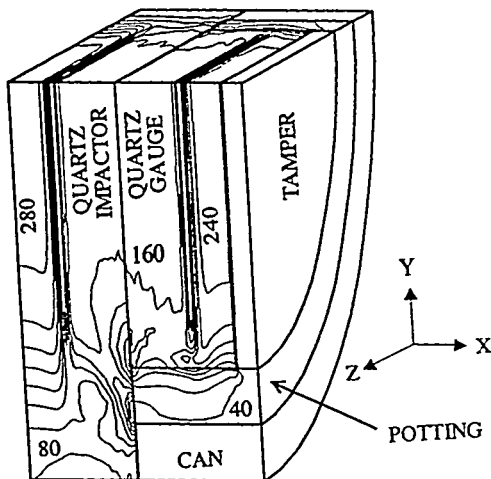


FIGURE 2. A quarter section of the finite element model for a fully electrode quartz gauge with can spacing $L/2$ approximately 0.7 μ second after impact. The component materials of the gauge and impactor are labeled, with Hysol epoxy being used for the potting material in the simulation. Contours of electric field magnitude are labeled from 40 kV/cm to 280 kV/cm.

A sample comparison of measured and calculated gauge current for a fully electrode gauge loaded at a stress of about 10 kbar is shown in Fig. 3. The observed current pulse typically shows more noise than seen in prior work due to improved higher frequency recording.

As can be seen, the calculated gauge current agrees very well with the measure current until near the end of the pulse. The rounding of the calculated current is due to wave dispersion caused by the finite element discretization and artificial viscosity used in SUBWAY. As a result the wave reflection from the tamper causes the computed current to be lower than observed in the actual shock event. The observed behavior is

representative of all the numerical simulations of gauge response conducted.

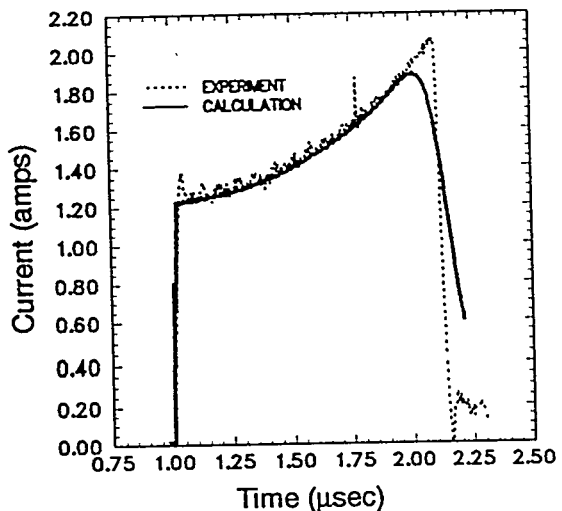


FIGURE 3. Experimental and calculated current pulses are compared for an experiment at about 10 kbar. Generally good agreements are observed, but certain features, particularly at late time, require more refined calculations.

Simulations of current pulses were carried out for four different fully electrode gauge configurations. At the same stress of 10 kbar, current pulses, stress distributions and electric field distributions were determined for two can spacing distances (L and $L/2$) and for two different epoxies (Hysol and alumina-loaded epoxy). The computed current pulses are shown in Fig. 4 in which the plotted currents are restricted to the values that show the initial current jump and the final values of the current at wave transit time.

The effects of both the epoxy and can spacing are readily apparent. The epoxy effect is a direct result of differences in dielectric constant. The can spacing effect is a result of electric field fringing within the gauge resulting from the proximity of the can to the edge of the disk.

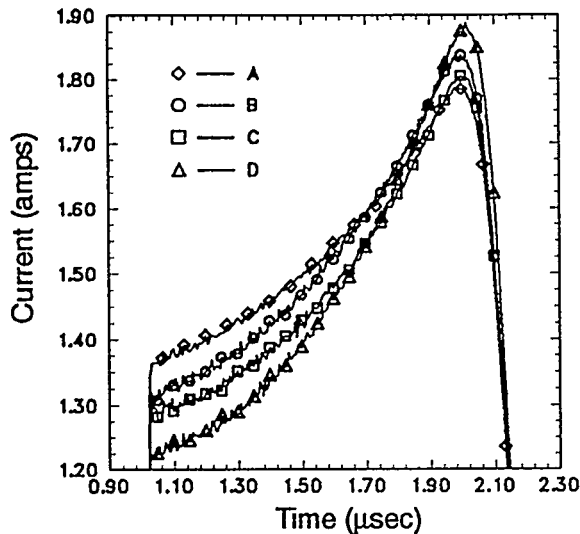


FIGURE 4. Calculated gauge currents for the fully electrode gauge configuration. The plot is restricted to the values that show the initial jump and final calculated values of the quartz gauge current. The curve labeled A corresponds to alumina loaded epoxy potting and a can spacing of L. The curve labeled B corresponds to alumina loaded epoxy potting and a can spacing of L/2. The curve labeled C corresponds to Hysol epoxy potting and a can spacing of L. The last curve, labeled D, corresponds to a calculation with Hysol epoxy potting and a can spacing of L/2.

As can be seen in this figure, the initial current jump depends on can spacing and potting material. For fixed can spacing the simulations show that the initial current jump is higher for the Hysol epoxy potting. Since the dielectric constant for the Hysol epoxy is lower than that for the alumina loaded epoxy these results indicate that the initial current jump decreases with increasing dielectric constant of the potting material. This result is a consequence of larger electric field fringing resulting from higher dielectric constant.

Figure 5 shows an enlargement of the electric field distribution in the outer region of the disk. Three different lines of constant field are shown

for can spacings of L, L/2 and L/4. There is a clearly discernible effect on field distribution caused by the can spacings. The field distribution is consistent with the current pulse predictions.

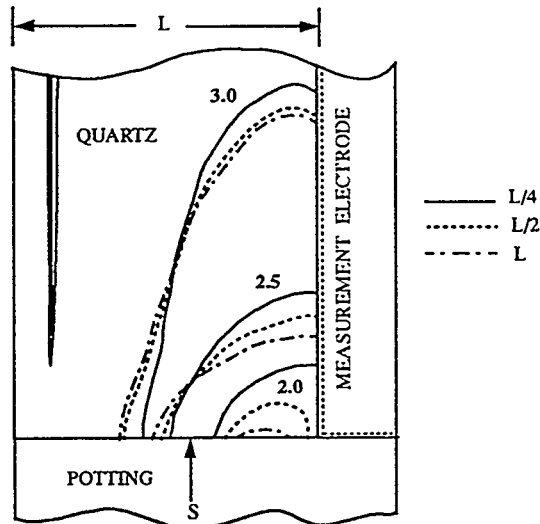


FIGURE 5. Contours of the electric field magnitude in a section of the quartz gauge, approximately 0.7 μsecond after impact.

CONCLUSIONS

The present work has shown that the SUBWAY code can be used as a quantitative tool for study of the physics and phenomenology of piezoelectric gauges. The code will prove particularly useful in study of the shorted guard ring gauges.

REFERENCES

1. Graham, R. A., Neilson, F. W., and Benedick, W. B., *J. Appl. Phys.* 36, 1775-1783 (1965).
2. Montgomery, S.T. and Chavez, P. F., *Basic Equations and Solution Method for the Calculation of the Transient Electromechanical Response of Dielectric Devices*, Sandia National Laboratories Report, SAND86-0755, June 1986.
3. Taylor, L.M. and Flanagan, D.P., *PRONTO 3D: A Three-Dimensional Transient Solid Dynamics Program*, Sandia National Laboratories Report, SAND87-1912, March 1989.
4. Tiersten, H.F., *Linear Piezoelectric Plate Vibrations*, New York: Plenum Press, 1969, ch. 7, pp. 51-61.
5. Graham, R.A., *Physical Review*, 6, 4779-4793 (1972).